Particle Size of Mechanically Alloyed $La_{0.5}Sr_{0.5}Fe_{0.5}Mn_{0.25}Ti_{0.25}O_3$ Powders Prepared with the Assistance of Ultrasonic Irradiation

Azwar Manaf[1] & Mas Ayu Elita Hafizah[1]

[1] Faculty of Maths and Natural Science, Graduate Program of Materials Science, Universitas Indonesia, Indonesia

Correspondence: Azwar Manaf, Graduate Program of Materials Science, Faculty of Maths and Natural Science, Universitas Indonesia, kampus UI, Jl. Salemba Raya No. 4, Jakarta 10430, Indonesia. Tel: 62-213-927-554. E-mail: azwar@ui.ac.id

Abstract

This paper reports the particle size characterisation of mechanically alloyed $La_{0.5}Sr_{0.5}Fe_{0.5}Mn_{0.25}Ti_{0.25}O_3$ prepared with the assistance of a high-power ultrasonic treatment. After a solid-state reaction on quasi-crystalline powders at 1000°C for 3 hour, the presence of a single phase was confirmed by X-ray Diffraction (XRD). It was found that powder materials derived from mechanical alloying and successive sintering have several disadvantages, namely, that the particle morphology is seldom controllable and results in large variations in the particle size and distribution. A significant improvement in both particle size and distribution was obtained upon subjecting the mechanically milled powder materials to an ultrasonication treatment for a relatively short period of time. As determined by a particle size analyser, the mean particle size gradually decreased from the original size of 6.23 to 1.13μm. A narrow size variation was also observed by Scanning Electron Microscope (SEM). The line broadening analysis by XRD revealed that the particles consist of nanocrystallites with an average size of ~ 22-26 nm. These results indicate that the sintering of mechanically milled particles followed by a high-power ultrasonication treatment promotes the formation of particles containing nanocrystals.

Keywords: mechanical alloying, sonochemical synthesis, particle size distribution, nanoparticles

1. Introduction

Perovskite lanthanum manganites, especially those doped $LaMnO_3$ (LMO), have shown significant potential for application in the field of magnetic electronic functional materials (Zi et al., 2009). Structural modification either through doping of La with Ca, Sr, and Ba (Pissas, Kallias, Hofmann, & Tobbens, 2002; Grossin & Noudem, 2004) or Mn with Fe, Cu, and Ti (Ahn, Wu, Liu, & Chien, 1997; Li et al., 2006; Kallel, Oumezzine, & Vincent, 2008) have been reported to induce electromagnetic properties such as giant magneto resistance (GMR) or colossal magneto resistance (CMR) (Haghiri-Gosnet & Renard, 2003; Ramirez, 1997). Another potential application is in the area of radar-absorbing materials (RAM) (Gama, Rezende, & Dantas, 2011). A partial substitution of La with Sr or Mn with Fe gives rise to new properties, in addition to the GMR or CMR, in which the substituted LMO has the ability to absorb electromagnetic waves, especially in the ultra-high frequency range (GHz) (Zhou et al., 2009; Zhou et al., 2007).

The use of telecommunication and information technologies is currently experiencing rapid growth. With the introduction of advanced technologies, such as various kinds of electronic media and information technologies, the use of electromagnetic waves (EM) over a broad range of frequencies is becoming more important. Consequently, the need to find new absorbing materials is the goal of many research activities.

Our current research interest focuses on a series of ion-substituted LMO compounds, with the structure of $(La_{1-x}Sr_x)(Fe_{0.5}Mn_{0.25}Ti_{0.25})O_3$ with x = 0, 0.25, 0.5, 0.75 and 1.0, for application as high-frequency microwave absorber materials. Our studies include the preparation of nanocrystalline-based materials to improve their microwave absorption characteristics. Reports have shown that processing routes such as conventional mechanical alloying and solid-state reaction (Suryanarayana, 2001) can be utilised for the preparation of nanomaterials. In addition to these conventional approaches, other methods such as sol-gel (Chen, Nass, & Vilminot, 1997), co-precipitation (Rashad, Zaki, & El-Shall, 2009) and hydrothermal (Wang et al., 2011) have also been used for nanomaterial synthesis. However, in most cases, the mechanical alloying and milling route

requires a relatively long milling time - from tens to hundreds of hours to obtain fine powders. In addition, the final product may be significantly contaminated by unwanted materials. Similarly, chemical routes such as the sol-gel process may be considered less effective, especially when a large amount of material is produced, because a significant amount of unwanted materials remains as waste.

We devised an alternative route for overcoming the unnecessarily long milling time and excessive contamination to prepare fine powder materials with a homogeneous particle size distribution. The characterisation of the resulting crystallites and particles is discussed in this report. Beginning with quasi-crystalline materials obtained from mechanical alloying and successive sintering to induce crystallisation, a further refinement of the particle size is afforded by the application of a high-power sonicator.

2. Experimental Work

Designated $(La_{1-x} Sr_x) (Fe_{0.5}Mn_{0.25}Ti_{0.25}) O_3$ with x = 0, 0.25, 0.75 and 1.00 compositions were prepared using a conventional milling technique. Stoichiometric quantities of analytical-grade $MnCO_3$, $SrCO_3$, Fe_2O_3, TiO_2 and La_2O_3 precursors with a purity of greater than 99% were mixed and milled using a planetary ball mill to a powder weight ratio of 10:1 for up to 70 hours. All samples were characterised by powder X-ray diffraction (XRD) using Philips PW3710 diffractometer with CoK_α radiation (λ = 1.78896 Å). In all cases, powders obtained after 10 hours of milling time were found to be highly deformed materials, as indicated by the absence of Bragg diffraction peaks and the presence of broad and diffuse peaks by XRD analysis. Thus, these powders may be considered quasi-crystalline or amorphous phases. A small quantity of milled $La_{0.5}Sr_{0.5}Fe_{0.5}Mn_{0.25}Ti_{0.25}O_3$ powders was removed from time to time for mean particle size characterisation during the 70 hr milling process.

One portion of mechanically alloyed powders obtained after 10 hours of milling time were investigated further to determine the effects of ultrasonic irradiation on the particle size refinement. The refinement was performed in the following manner: after mechanically milling for 10 hours, powders were successively sintered at 1000^oC for 3 hours to produce crystalline materials. The sintered powders were then dispersed in distilled water to form powder solutions of various concentrations. The solutions were then irradiated ultrasonically using a 1.2 kW sonicator operating at 40 kHz for different periods of time up to 70 hrs. The suspensions were then collected by precipitation using a centrifuge. The particle size was evaluated using a Helos simpatec particle size analyser for micron-sized particles and a Zeta nanosizer analyser for nano-sized particles. Additional XRD analysis was performed to determine the mean crystallite size. In this case, un-overlapping diffracted peaks were selected, and reliable line broadening data were obtained using the step-scanning mode. Intensity data were recorded for each 0.005° step using a 2-second scanning time, and the mean crystallite size was derived from *Scherrer's* formula (Cullity, 1976). The diffraction peak width of the test sample, B_s, was calculated from the full-width at half-maximum (FWHM), whereas the true width, B, was determined using Equation 1. Finally, the mean crystallite size was obtained from Equation 2,

$$B = (B_s - B_0)^{1/2} \tag{1}$$

$$d = 0.9 \lambda / B.Cos \theta \tag{2}$$

where d is the mean crystallite size, λ is the X-ray wavelength, θ is the Bragg angle, and B_0 is the FWHM of a standard sample that takes into account the instrumental broadening correction. A correction factor due to lattice strain was not utilised in the analysis. Microstructural examination of the samples was taken from fracture surfaces of the bulk samples using JEOL JSM-5310LV and JED-2300 scanning electron microscopes (SEM).

3. Results and Discussion

3.1 Effect of Milling Time on the Mean Particle Size

The fit XRD profile of a $La_{0.5}Sr_{0.5}Fe_{0.5}Mn_{0.25}Ti_{0.25}O_3$ sample prepared after 10 hours of mechanical alloying followed by sintering at 1000^oC for 3 hours is shown in Figure 1. The resulting profile of the residue shows almost no intensity over the entire diffraction angle range.
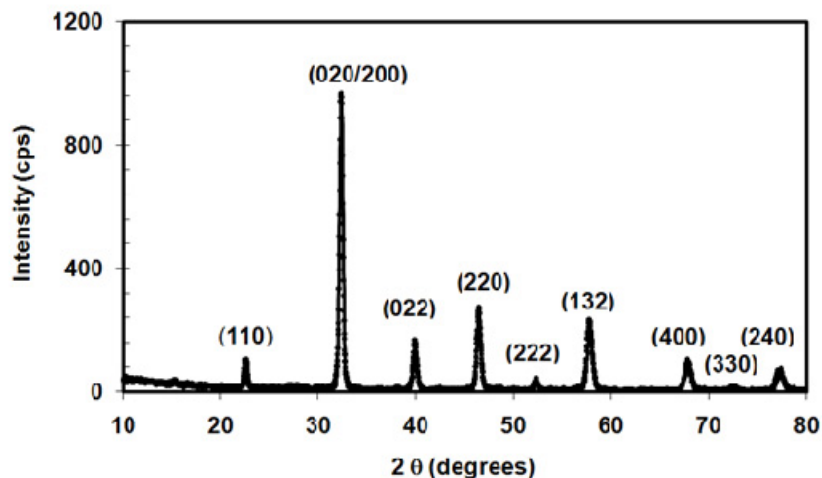
Figure 1. XRD trace of $La_{0.5}Sr_{0.5}Fe_{0.5}Mn_{0.25}Ti_{0.25}O_3$ prepared by mechanical alloying and sintering at 1000^oC for 3 hours
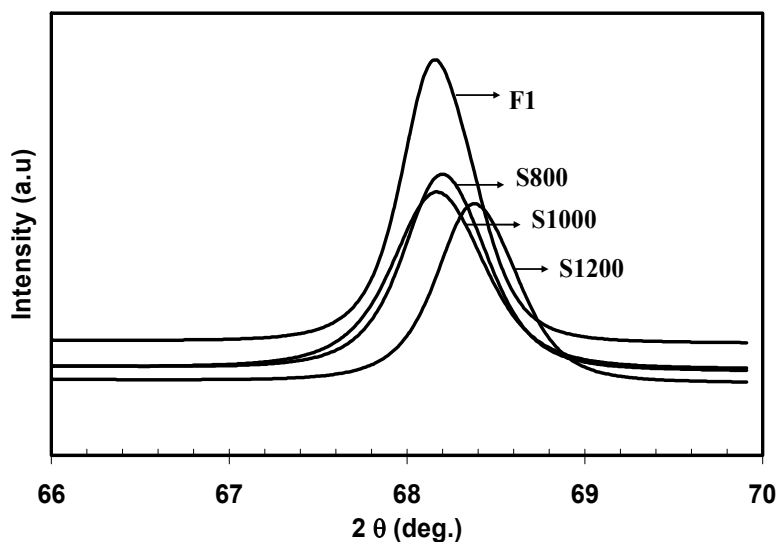
Figure 2. Plot of diffracted intensities of mechanically alloyed $La_{0.5}Sr_{0.5}Fe_{0.5}Mn_{0.25}Ti_{0.25}O_3$ powders after 10 hrs of milling time and sintered at 800^oC (S800), 1000^oC (S1000) and 1200^oC (S1200) for 3 hours and that of the sample S1000 with additional treatment ultrasonically (F1)

The convergent fitting process parameter was obtained with an acceptable χ^2 value of 1.24. The trace matches with the peaks of a Perovskite $LaMnO_3$ structure, despite a small shift in the peak positions due to the presence of a partial Sr ion substitution for La, in addition to Fe and Ti ion substitutions for Mn. Thus, the material is a single phase within a 4 % uncertainty for the phase fraction (Cullity, 1976). Similarly, the XRD traces of sintered powders obtained using sintering temperatures in the range of 800-1200 ^oC also exhibit a pattern similar to that of the $LaMnO_3$ phase. In addition, all XRD traces consistently exhibit diffraction line broadening. Figure 2 compares the diffraction intensity of the (400) peak for sintered powders obtained by step scanning in the range of 66-70 ^{o}.
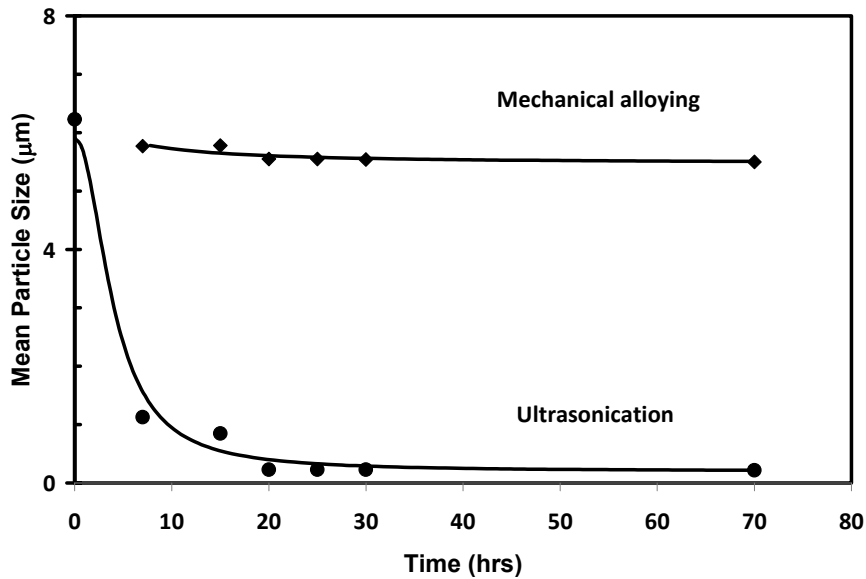
Figure 3. Comparison of mean particle size of powders prepared by conventional mechanical alloying with that of powders subject to ultrasonication. The ultrasonic irradiation was applied to crystallised mechanically alloyed powders
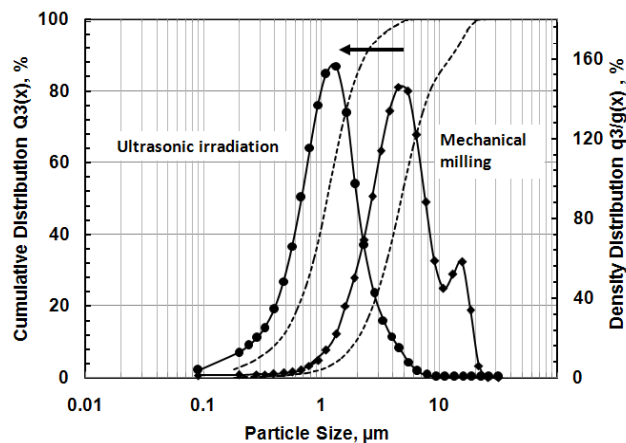

Figure 4. Particle size distribution of $La_{0.5}Sr_{0.5}Fe_{0.5}Mn_{0.25}Ti_{0.25}O_3$ powders prepared by conventional mechanical alloying and that of the powder subject to ultrasonication, demonstrating a significant size reduction due to ultrasonication treatment

We performed the particle size characterisation of mechanically milled and successively sintered materials using a particle size analyser. We observed that during the early stages of the milling process, the particle size increases due to the incorporation of material components, and it then progressively decreases until it plateaus after 10 hrs of milling time. The long-term mechanical treatment during the advanced stage of the process causes the particles to experience embrittlement due to the accumulation of internal stresses. Continuous plastic deformations of the brittle particles cause a further reduction in the particle size.

The evolution of the mean particle size of powder samples of mechanical milling after 10 hrs milling time is shown in Figure 3. The results indicate that particle size approaches a limit as the milling times is increased to 70 hours. There is no significant reduction in the mean particle size of mechanically alloyed powders during this period of time. The mean particle size after 70 hours of milling is 5.5 μm, which is only 0.73 μm smaller than that of the powder obtained after 10 hours of milling (time zero for the graphs in Figure 3). This finding indicates that a further decrease in the particle size results in an increase in the particle's fracture resistance, which, in turn,

causes the particles to become agglomerated.

Based on these results, we induced the de-agglomeration of the particles by subjecting sintered materials obtained after 10 hours of mechanical alloying to a powerful ultrasonication treatment. The results shown in Figure 3 demonstrate that the mean particle size is reduced to ~ 1.13 μm after 7 hours of sonication treatment. Extending the sonication time to 20 hours leads to a further decrease in the mean particle size to 0.23 μm. In addition to the mean particle size, the typical particle size distribution for materials obtained by mechanical milling is demonstrated in Figure 4. The bimodal curve indicates that the suspended particles in the dispersant media are inhomogeneous, despite sample already de-agglomerated by the normal ultrasonic treatment. The curve with the dashed line demonstrates that all particles are below approximately 20 μm in size. This behaviour is different from the results obtained for the powders subjected to ultrasonication, which show a particle size of less than 7 μm and a monomodal spectrum with a narrower particle size distribution. The mean particle size of ~ 1.13 μm is clearly much smaller.

3.2 Effects of Sintering Temperature on the Mean Crystallite Size

It is well-accepted that the line broadening of diffraction peaks is caused by fine crystallites sizes, crystal defects and induced microstrains, in addition to instrumental broadening (Samaila, Hashim, Yusof, & Abbas, 2010). The measured FWHM values of the diffraction peaks were calculated from Figure 2 and used to estimate the mean crystallite size for samples with a quasi-crystalline structure that were sintered at different temperatures to induce crystallisation. The mean particle and crystallite sizes for these samples are provided in Table 1. The table also includes the mean size for the sample subjected to the ultrasonication treatment in addition to the mechanical treatment.

If microstrain is neglected, values for mean crystallite size in the range of 20-26 nm were found. It is also noted that with the exception of the ultrasonically treated sample, the mean crystallite size for all samples was approximately 200-300 times smaller than that of the respective mean particle size. Moreover, although the mean particle size was much smaller for the ultrasonically treated sample in comparison to the first three, the mean crystallite size remained nearly the same. This result implies that there is no direct relation between the particle and crystallite sizes and that sintering temperatures do not significantly influence the mean size of the crystallite in the particles.

Table 1. Mean particles and crystallite sizes for crystallised samples

Sintering Temp.	Mean Size	
(°C)	Particles (nm)	Crystallites (nm)
1200	5380	23
1000	6230	20
800	4770	21
with additional treatment ultrasonically		
1000	1130	26

The SEM micrograph of the fracture surface for a loosely compacted and sintered sample is provided in Figure 5, which reveals that the particles are nearly spherical in shape and exhibit clean particle edges.
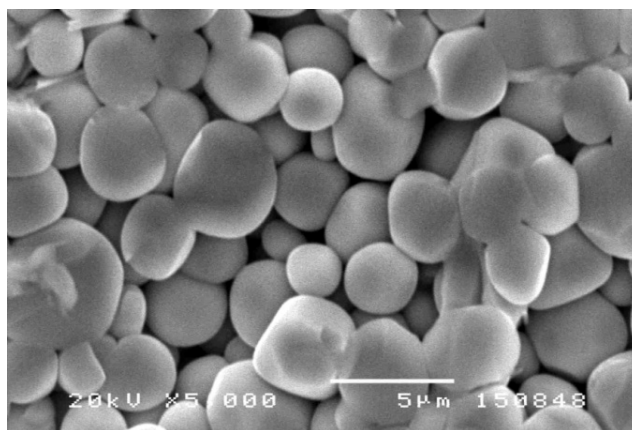
Figure 5. SEM image of the fracture surface of $La_{0.5}Sr_{0.5}Fe_{0.5}Mn_{0.25}Ti_{0.25}O_3$ sample prepared by mechanical alloying and sintering at 1200^oC

Based on the visual estimation of the particle size from Figure 5, the sample has a mean particle size of approximately 2 to 5 μm. The SEM estimation is close to the value calculated from the particle size distribution shown in Figure 3. Larger particles can be clearly seen in micrograph and represent clusters containing a number of particles. These clusters may be de-agglomerated further to a free-standing particle using a higher power sonicator.

We employed a 1.2 kW sonicator for the ultrasonic treatment of sintered powders to study the effect of the ultrasonication treatment on the shape and morphology of the particles. Based on the particle size evaluation, after more than 20 hrs of ultrasonic treatment, the mean particle size was reduced to ~ 220 nm, which is far below the mean particle size of the as-milled powders (Figure 3). Moreover, the shape morphology changed from that of spherical particles with clean edges to almost equiaxed particles. A SEM micrograph of a synthesised sample subjected to the ultrasonication treatment is shown in Figure 6. The image reveals the morphology and size of nanocrystallites and the presence of particles that exist as aggregates of fine grains. This may be compared with the SEM image of the as-milled particles in Figure 5. It is clear that the additional ultrasonication treatment of mechanically alloyed powders is quite effective, not only in reducing the particle size, but also in changing the shape of the particles and producing a significant improvement in their size distribution.
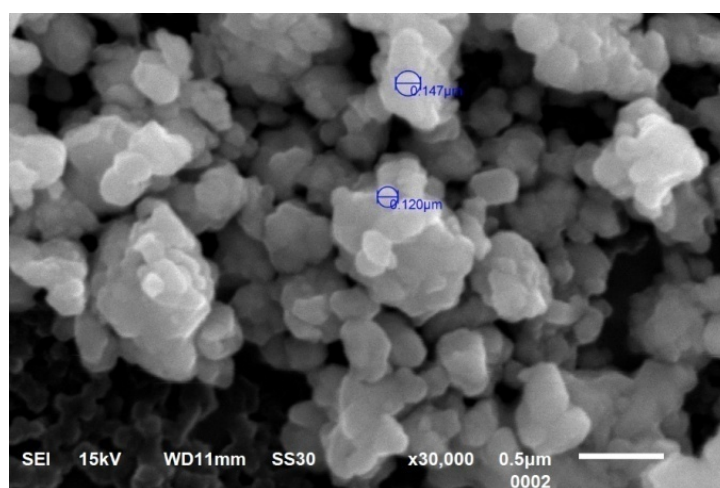

Figure 6. High-resolution SEM image of $La_{0.5}Sr_{0.5}Fe_{0.5}Mn_{0.25}Ti_{0.25}O_3$ powders after sonication demonstrating the presence of nanocrystals

Despite our limited understanding of the physical processes created by ultrasonic irradiation in the presence of liquids, it has been reported that the ultrasonication treatment commences with the creation of thousands of cavitation bubbles, which eventually result in an implosive collapse. This collapse of cavitations is accompanied by a high release of energy, which itself produces local sound waves with pressures of hundreds of atmospheres and transient hot spots with temperatures of several thousand K (Gedanken, 2004). It was also reported that shock waves generated by cavitations in liquids containing metal particles drives the particles together at extremely high speeds, causing a series of unavoidable collisions among the particles (T. Prozorov, R. Prozorov, & Suslick, 2004). This results in severe destruction of the particles and forces large grains into fragments of particles and grains of smaller sizes. As the grain boundaries are the most reactive areas and are present at a high energy state, they are considered to be the most vulnerable part of the system. Thus, the local pressure generated by the bubbles is assumed to be responsible for splitting the particles into fine crystallites, whereas the collisions among the particles are responsible for the resulting particle shape.

The above results suggest that there is a significant difference between the mean size of the particle and crystallites. Mechanical alloying by ball milling results in heavily deformed particles that form alternate layers with almost free crystallites. This is evident by the absence of diffraction peaks in the XRD trace for a sample prepared after 10 hours of mechanical alloying. The sintering of this material induces crystallisation, transforming the amorphous material into a poly-crystalline material. We believed that upon sintering of the mechanically alloyed powder materials, the solid-state reaction and crystallisation occur, which promote the formation of particles containing nanocrystals. Upon further treatment by ultrasonic irradiation, the mean size of the particles containing nanocrystals is significantly reduced.

4. Conclusion

The preparation and evaluation of mechanically alloyed $La_{0.5}Sr_{0.5}Fe_{0.5}Mn_{0.25}Ti_{0.25}O_3$ powders was discussed. The conventional milling produced an inhomogeneous particle size distribution, with an average particle size of ~ 6 μm. However, a much finer crystallite size of ~ 20-26 nm was observed for these particles. When the mechanically alloyed particles were subjected to an additional ultrasonication treatment, even smaller particles with a mean particle size below 200nm were obtained, although the mean crystallite size did not change. We conclude that mechanical alloying coupled with ultrasonication can be an alternative route for the preparation of fine and homogeneous powder materials leading to nanoparticle-based materials.

References

Adriana, M. Gama, Mirabel, Rezende, & Christine, C. Dantas. (2011). Dependence of microwave absorption properties on ferrite volume fraction in MnZn ferrite/rubber radar absorbing materials. *Journal of Magnetism and Magnetic Materials, 323*, 2782–2785. http://dx.doi.org/10.1016/j.jmmm.2011.05.052

Aharon, Gedanken. (2004). Using sonochemistry for the fabrication of nanomaterials. *Ultrasonics Sonochemistry, 11*, 47–55. http://dx.doi.org/10.1016/j.ultsonch.2004.01.037

Ahn, K. H., Wu, X. W., Liu, K., & Chien, C. L. (1997). Effects of Fe doping in the colossal magnetoresistive $La_{1-x}Ca_xMnO_3$. *J. Appl. Phys., 81*(8), 5505-5507. http://dx.doi.org/10.1063/1.364584

Chen, Y. F., Nass, R., & Vilminot, S. (1997). Seeding effects in the sol–gel preparation of lead zirconate titanate (PZT) powders. *J. Sol–Gel Sci. Technol., 8*, 385–389. http://dx.doi.org/10.1007/BF02436870

Cullity, B. D. (1976). *Elements of X-ray Diffraction*. Addison-Wesly Publishing Co. Inc.

Grossin, D., & Noudem, J. J. (2004). Synthesis of fine $La_{0.8}Sr_{0.2}MnO_3$ powder by different ways. *Solid State Sciences, 6*, 939-944. http://dx.doi.org/10.1016/j.solidstatesciences.2004.06.003

Haghiri-Gosnet, A. M., & Renard, J. P. (2003). CMR manganites: physics, thin films and devices. *J. Phys. D: Appl. Phys., 36*, 127-150. http://dx.doi.org/10.1088/0022-3727/36/8/201

Kallel, N., Oumezzine, M., & Vincent, H. (2008). Neutron-powder-diffraction study of structural and magnetic structure of $La_{0.7}Sr_{0.3}Mn_{1-x}Ti_xO_3$ (x = 0, 0.10, 0.20, and 0.30). *Journal of Magnetism and Magnetic Materials, 320*, 1810-1816. http://dx.doi.org/10.1016/j.jmmm.2008.02.106

Li, W. J., Zhao, B. C., Ang, R., Song, W. H., Sun, Y. P., & Zhang, Y. H. (2006). Structural, magnetic, and transport properties in $La_{(2+4x)/3}Sr_{(1-4x)/3}Mn_{1-x}Cu_xO_3$ ($0 \leq x \leq 0.20$) system. *Journal of Magnetism and Magnetic Materials, 302*, 473–478. http://dx.doi.org/10.1016/j.jmmm.2005.10.008

Pissas, M., Kallias, G.., Hofmann, M., & Tobbens, D. M. (2002). Crystal and magnetic structure of the $La_{1-x}Ca_x MnO_3$ compound (x = 0.8, 0.85). *Physical Review B, 65*, 064413-(1-9). http://dx.doi.org/10.1103/PhysRevB.65.064413

Ramirez, A. P. (1997). Colossal magnetoresistance. *J. Phys. Condens. Matter., 9*, 8171-8199. http://dx.doi.org/10.1088/0953-8984/9/39/005

Rashad, M. M., Zaki, Z. I., & El-Shall, H. (2009). A novel approach for synthesis of nanocrystalline $MgAl_2O_4$ powders by co-precipitation method. *J. Mater. Sci., 44*, 2992–2998. http://dx.doi.org/10.1007/s10853-009-3397-8

Samaila, Bawa Waje, Mansor, Hashim, Wan, Daud Wan Yusoff, & Zulkifly Abbas. (2010). X-ray diffraction studies on crystallite size evolution of $CoFe_2O_4$ nanoparticles prepared using mechanical alloying and sintering. *Applied Surface Science, 256*, 3122–3127. http://dx.doi.org/10.1016/j.apsusc.2009.11.084

Suryanarayana, C. (2001). Mechanical alloying and milling. *Progress in Materials Science, 46*, 1-184. http://dx.doi.org/10.1016/S0079-6425(99)00010-9

Tanya, Prozorov, T., Prozorov, R., & Suslick, K. S. (2004). High Velocity Interparticle Collisions Driven by Ultrasound. *J. AM. Chem. Soc., 126*, 13890-13891. http://dx.doi.org/10.1021/ja049493o

Wang, Z. Z., Xie, Y. Y., Wang, P. H., Ma, Y. Q., Jin, S. W., & Liu, X. S. (2011). Microwave anneal effect to magnetic properties of $Ni_{0.6}Zn_{0.4}Fe_2O_4$ nano-particles prepared by conventional hydrothermal method. *Journal of Magnetism and Magnetic Materials, 323*, 3121-3125. http://dx.doi.org/10.1016/j.jmmm.2011.06.068

Zhou, K. S., Xia, H., Huang, K. L., Deng, L. W.,Wang, D., … & Gao, S. H. (2009). The microwave absorption properties of $La_{0.8}Sr_{0.2}Mn_{1-y}Fe_yO_3$ nanocrystalline powders in the frequency range 2–18GHz. *Physica B, 404*, 175-179. http://dx.doi.org/10.1016/S1003-6326(07)60205-2

Zhou, K. S, Wang, D., Huang, K. L., Yin, L. S., Zhou, Y. P., & Gao, S. H. (2007). Characteristics of permittivity and permeability spectra in range of 2-1 8 GHz microwave frequency for $La_{1-x}Sr_xMn_{1-y}B_yO_3$ (B=Fe, Co, Ni). *Trans. Nonferrous Met. Soc. China, 17*, 1294-1299. http://dx.doi.org/10.1016/S1003-6326(07)60265-9

Zi, Z. F., Suna, Y. P., Zhua, X. B., Haoa, C. Y., Luoa, X., Yanga, Z. R., … & Songa, W. H. (2009). Electrical transport and magnetic properties in $La_{0.7}Sr_{0.3}MnO_3$ and $SrFe_{12}O_{19}$ composite system. *Journal of Alloys and Compounds, 477*, 414-419. http://dx.doi.org/10.1016/j.jallcom.2008.10.027